Numerical simulation of airflow around buildings

F. WENIG, C. HESCHL, P. KLANATSKY & TH. DRAGOSITS
University of Applied Sciences Burgenland, Pinkafeld, Austria

ABSTRACT: Computational Fluid Dynamics (CFD) is a commonly accepted tool for studying the wind flow over complex terrain and buildings. But an accurate prediction of the flow field implies a correct reproduction of the turbulent quantities and consequently the right choice of the turbulence model. Due to the highly dissipative behavior of the RANS based turbulence models they are not able to trigger unsteady motion (e.g. flow downstream of buildings) unless the flow instabilities are strong. For this reason model approaches which are able to adjust the turbulence length scale so that the macroscopic fluctuations are resolved will be more and more used. This approach of a URANS model is denoted Scale-Adaptive Simulation (SAS) and requires less computational effort compared to the Large Eddy Simulation (LES) method. Although the theoretical advantage for flow around building simulations is well founded only minor practical experience exists. Therefore, in this work the Scale-Adaptive Simulation model is investigated by validating it with experimental data from wind tunnel measurements. Beside the SAS model, the standard k-ε and various k-ε-v^2-f and k-ω turbulence models are also applied. It shows, that the SAS turbulence model agrees well with the experimental data. The standard k-ε model produces too much turbulent kinetic energy which is transported downstream and suppressing an unsteady solution. The high turbulence level dominates the turbulent viscosity distribution in the wake so that the standard k-ε turbulence model lead to comparable results but with substantial lower computational effort.

1. INTRODUCTION

In the course of the evaluation of wind power resources a detailed prediction of the flow around buildings is necessary. For this Computational Fluid Dynamics (CFD) is often used in the practical design stage. Because of the computational economy the simulations are generally based on the Reynolds-averaged Navier Stokes equations (RANS). Thereby the CFD-user is exposed to the risk of oversimplifying the turbulent processes and consequently he is not able to correctly reproduce the key phenomena encountered in wind and environmental engineering. Especially complex flows such as impingement, bluff body wake and unsteady three dimensional boundary layer separations are affected. The last ones contain geometry induced flow oscillations which can significantly alter the behavior of important parameters such as Reynolds-stresses, turbulent kinetic energy and the dissipation rate (Haase et al., 2009). In principle statistical turbulence models are able to better reproduce such unsteady flows if the turbulence is statistically stationary or if a unique spectral gap which separates the frequency band of the unsteady basic flow from the frequency band of the turbulent fluctuations exists. For the last case unsteady RANS (URANS) models assume that all turbulent fluctuations develop only in the high frequency (low scales) range. Moreover, the unsteady resolved frequency range should lie outside of the modeled turbulence spectrum. In many practical applications both demands are not fulfilled so that an alternative approach to the URANS modeling must be considered.

Because of the deficiencies of the URANS method Spalart et al. (1997) and Strelets (2001) proposed the Detached Eddy Simulation (DES) methodology. DES combines the RANS and Large Eddy Simulation (LES) techniques whereby the turbulent length scale is limited by the grid spacing so that the eddy viscosity is reduced and the three-dimensional turbulent structures in the detached flow region can be directly resolved. The original DES concept was intended for flows with a clear separation of attached and detached flow regions, where the RANS technique would be active in the attached flow region and the LES

technique in the detached zone. The use of the LES method leads to high computational costs and to a grid dependency of the results. Motivated by this fact Menter and co-workers (e.g. Menter & Egorov, 2005, 2009) developed a scale-adaptive simulation (SAS) method which uses an additional production term in the ω-equation which considers unsteady effects. For the detecting of the flow unsteadiness the Karman length scale is introduced. The Karman length scale is based on the ratio of the first to the second velocity gradients and is thereby smaller for an unsteady velocity profile than for a steady-state flow (Davidson, 2006). The additional source term contains the ratio between the modeled turbulent length scale and the Karman length scale so that in unsteady flow regions the specific dissipation rate increases and hence the turbulent viscosity decreases. This kind of modification adapts dynamically the standard URANS equations so that more unsteady structures in the flow field can be resolved. Benchmark tests about flow around wall mounted cubes, airfoils, wings, car mirror etc. show that the SAS method can clearly improve the computational results and that this method seems to be a promising alternative to the conventional RANS and URANS approaches (Haase et al., 2009).

To analyze the potential of the SAS model for flow around buildings three different test cases - the flow around a 3D cube, a 3D cube array and a 3D building array – were investigated with RANS, URANS and SAS. The used turbulence models depend on the three methods. The RANS models are based on the conventional eddy viscosity concept (EVM) without realizability constraint so that an over production of the turbulent kinetic energy in the stagnation point region arise. Consequently downstream of the obstacles a higher turbulent viscosity can be expected. In contrast to the RANS method all used URANS models include modifications to limit the production of the turbulent kinetic energy in the stagnation point area.

For the RANS and URANS method k-ε and k-ω based turbulence models are used. Past investigations have shown that models which use an elliptic relaxation approach, which accounts for wall blocking effects affecting the Reynolds-stresses, has a very good performance for separated, impinging and bluff body flows (e.g. Lopes da Costa et al., 2007; Sveningsson, 2003; Cokljat et al., 2003; Durbin, 1995a). Therefore k-ε-v^2-f based turbulence models are also used for the RANS and URANS calculations. For the SAS investigations only one basis model – the k-ω shear-stress transport model (KW-SST) is used. All simulations were done with the commercial CFD-Code Fluent 14.5 (cf. Heschl et al., 2010).

2. DESCRIPTION OF THE APPLIED TURBULENCE MODELS

2.1 TURBULENCE MODELS FOR RANS SIMULATION

The RANS simulations were done with the standard k-ε turbulence model with enhanced wall treatment (SKE) (Fluent, 2009), the k-ω baseline Model (KW-BSL) and the k-ε-v^2-f Model (V2F). In selected cases with coarse grid resolution in the near-wall region, the simulations with the SKE model were done with the standard wall function (Fluent, 2009). In contrast to the KW-SST turbulence model the KW-BSL model does not include the adverse pressure gradient correction in the defining equation of the turbulent viscosity. Hence for the KW-BSL model the turbulent viscosity is determined with Eq. (1) and the diffusion coefficient for the transport equation of the turbulent kinetic energy is changed from 1.176 to 2.0 (Menter, 1993).

$$\mu_t = \rho \alpha^* \frac{k}{\omega} \tag{1}$$

The V2F Model was implemented in Fluent via user-defined scalar interface (UDS). Because Fluent solves the additional transport equations segregated the code friendly k-ε-v^2-f version by Lien & Kalitzin (2001) was used. To avoid singularities in the governing equations at the solid walls the time scale and the length scale is limited by the following equations using Kolmogorov variables:

$$T = \max\left(\frac{k}{\varepsilon}, 6\sqrt{\frac{\nu}{\varepsilon}}\right) \quad L = C_L \max\left(\frac{k^{3/2}}{\varepsilon}, C_\eta \frac{\nu^{3/4}}{\varepsilon^{1/4}}\right) \tag{2}$$

2.2 URANS BASED TURBULENCE MODELS

The URANS simulations are based on the k-ω and k-ε-v^2-f models with realizability constraint to avoid the stagnation point anomaly. For this reason the KW-SST model with the original turbulent viscosity determination (Menter, 1994) was used instead of the KW-BSL model:

$$\mu_t = \frac{\rho k}{\omega} \frac{1}{\max\left[\frac{1}{\alpha^*}, \frac{S F_2}{a_1 \omega}\right]} \tag{3}$$

The k-ε-v^2-f model is extended by the "realizability" constrain proposed by Durbins time scale approach (Durbin, 1995b).

$$T = \min\left[\max\left(\frac{k}{\varepsilon}, 6\sqrt{\frac{\nu}{\varepsilon}}\right), \frac{C_{\lim} k}{\sqrt{6} C_\mu v^2 S}\right] \tag{4}$$

To avoid numerical instabilities the additional limit was only applied in the time scale determination for the turbulent viscosity and the dissipation rate (Sveningsson, 2003). For the model constant C_{lim} the value 0.6 was assumed. In this paper the k-ε-v^2-f model with the realizability constraint according equation (4) is labeled as V2F-RC.

2.3 SAS BASED TURBULENCE MODEL

All SAS simulations were done with the KW-SST based SAS turbulence model included in Fluent 14.5. In this paper the SAS results are denoted as KW-SST-SAS.

3. TEST CASES AND RESULTS

To investigate the performance of the RANS, URANS and SAS models the flow over a 3D cube (case A1-4 from the CEDVAL database), a 3D cube array (Brown et al., 2001) and a 3D building array (Meile, 2011 and Meile & Wimmer, 2011) were chosen. The RANS and URANS calculations reported below were performed with the coupled pressure-based solver and the second order discretization scheme for the convective and unsteady terms. For the SAS calculations the PISO algorithmus was used for the pressure-velocity coupling and the advection was approximated by central-differencing scheme. Due to the simple geometry in both cube cases a uniform hexahedral mesh could be used, with y^+-values of 1 for the grid line closest to the wall. The more complex building geometry for the third case was primarily realized by tetrahedral mesh with y^+-values for the wall attached cells of 1. For further investigations two additional grids of the building array with y^+-values of 30, out of tetrahedral (tet) as well as non-uniform hexahedral (hex) grid cells were generated. In all simulations the outlet was defined with pressure, the top side with symmetry and the bottom side with wall boundary condition. For the lateral domain side periodic boundary condition with zero pressure gradients were used in both cube cases, whereas symmetry condition was used in the building array case. To achieve a good convergence behavior the time step size for the URANS simulation was specified at 0.01 and for the SAS model at 0.001 seconds. In both cases the averaging time was about 6 seconds.

3.1 3D CUBE

To ensure a high resolution grid the computational domain consists of 272x143x180 grid cells in the x, y and z direction. The edge length of the cube is H=0.125 m and the computational domain ranges from x/H=-8 upwind and x/H=10 downwind. The height of the domain is limited with z/H=10 and the side boundaries are located at y/H=±5.5H.

The measured velocity distribution at x/H=-8 was used to determine the shear stress velocity (u_τ=0.2916 m/s) and the roughness length (z_0=0.000394 m). Based on the logarithmic law the inlet velocity distribution was determined ($u/u_\tau=1/\kappa \ln(z/z_0)$; Ehrhard, 1999). The turbulent kinetic energy and the dissipation rate were derived from the equilibrium condition between the production and dissipation ($k=u_\tau^2/\sqrt{c_\mu}$ with c_μ=0.09; $\varepsilon=u_\tau^3/(\kappa z)$ and $\omega=u_\tau/(\kappa \sqrt{c_\mu}\, z)$ with κ=0.4187; Ehrhard, 1999).

Fig. 1 provides a comparison of the predicted and measured x-velocity profiles and the levels of the turbulence kinetic energy downstream of the cube in the y=0 plane. It is surprising that all RANS models (SKE, KW-BSL and V2F) give similar results for both the velocity distribution and the turbulence. The reason for this outcome is the over prediction of the turbulent kinetic energy in the stagnation point as shown in Fig. 2. Consequently the turbulence in the wake is dominated from the stagnation point turbulence transported downstream and suppressing an unsteady solution. On the other hand, if the stagnation point anomaly is corrected as given in Eqs. (3) and (4), no turbulence is generated in the stagnation point region. Thus, less turbulence and thus less numeric dissipation allows the switch into unsteady flow (URANS modeling).

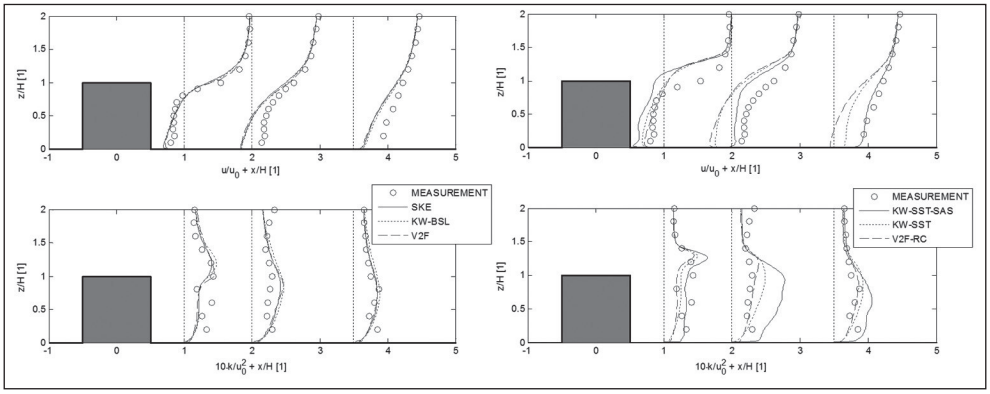

Fig. 1: x-velocity and kinetic energy distribution in the y=0 plane downstream of the cube (u_0=4.776 m/s). Left: investigated RANS models. Right: Investigated URANS and SAS models. (Heschl et al., 2010)

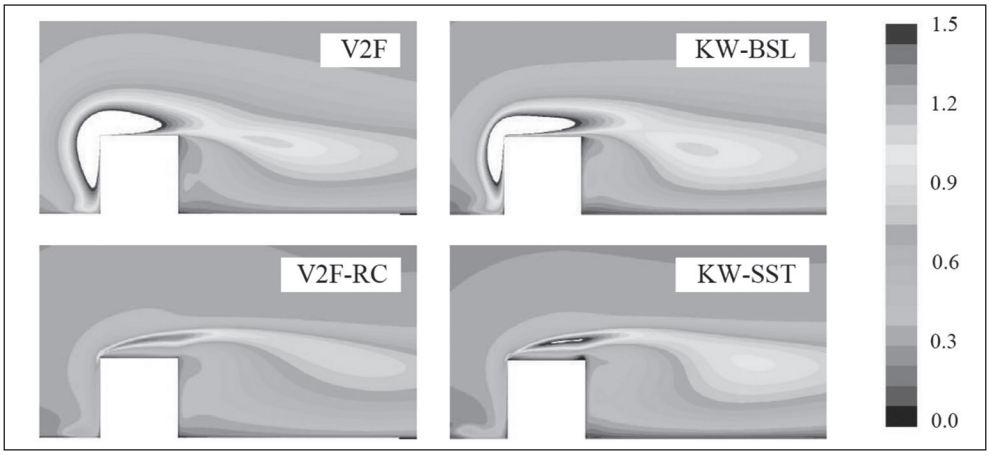

Fig. 2: Kinetic energy distribution in the evaluation plane y=0 (unit of the colorbar [m²/s²]). Top: RANS based models. Bottom: URANS based models. (Heschl et al., 2010)

Though the URANS models are able to predict the turbulent kinetic energy distribution more realistic (see Fig. 2) the results from the RANS models clearly better agree with the experimental data. It seems that the URANS models are not able to resolve the extent of the unsteady behavior of the basic flow correctly. A reason could be that no spectral gap between the frequency band of the unsteady basic flow and the turbulent fluctuations exists as discussed before.

Immediately downstream of the cube (x/H=1) the RANS models give the best agreement with the mean velocity measurements, on the other hand, the length of the recirculation zone is clearly overpredicted, because all RANS models underpredict the turbulence kinetic energy (and thus the flow dissipation) in the wake of the obstacle, despite the high turbulence kinetic energy computed in the stagnation point region. So all RANS models determine the turbulent production in the three dimensional wake insufficiently and overestimate the turbulent dissipation rate.

The additional source term in the KW-SST-SAS model reduces the turbulent viscosity and thus allows larger fluctuations in the wake than the URANS models. Therefore it can capture the flow recovery downstream of the separation zone in good agreement with the experimental data.

3.2 3D CUBE ARRAY

A detailed description of the wind tunnel experiments of the flow over a 3D cube array is given by Brown et al. (2001) so that only the important data needed for the computations are presented here. The experiment simulates neutrally stratified atmospheric boundary-layer flow over an array of 3D buildings. The array consists of sharp-edge cubes with a characteristic dimension of H=0.15 m. In the experiment 77 cubes were placed in an aligned array consisting of 11 rows of 7 cubes (the arrangement of the cubes is also described in Lien & Yee (2004)). To keep the computational effort low, the displayed domain was reduced to one row with 7 cubes. The domain spans from x/H=-5 to x/H=23 with the windward face of the first building placed at x/H=0. The height of the domain is z/H=8 and the width y/H=2. The velocity inlet profile was approximated with the power law $u/u_0=(z/H)^{\alpha}$. According to the experimental data the reference velocity was assumed with u_0=3 m/s and the exponent with α=0.16. The turbulence parameters for k, ε and ω were derived from the turbulence equilibrium ($k=u_\tau^2/\mathrm{sqrt}(c_\mu)$ with c_μ=0.09; $\varepsilon=u_\tau^3/(\kappa\, z)$ and $\omega=u_\tau/(\kappa\, \mathrm{sqrt}(c_\mu)\, z)$ with κ=0.4187; Ehrhard, 1999). Based on the experiments a friction velocity of u_τ=0.24 m/s was used. The number of grid cells was in x-direction 646, in y-direction 82 and in z-direction 98 so that the computational domain consists of about 5 million cells.

Fig. 3 to 6 provide a comparison of the predicted velocity profiles in x-direction and the levels of the turbulence kinetic energy. Analogous to the 3D cube all RANS based turbulence models give similar results. In addition both URANS models (KW-SST and V2F-RC) yield similar outcomes to each other. Especially between the first two cubes the RANS models give clearly better results than the URANS and the SAS solution. This corresponds to the observation of the 3D cube case where just behind the trailing edge (x/H=1) URANS and SAS models show also the largest deviations.

However between the cubes 5 and 6 the URANS models agree better with the experimental data, although the RANS models also show agreement with the experimental data. It is assumed that the unsteady behavior of the basic flow there is more distinct from the turbulent fluctuations as between the cubes 1 and 2. The SAS model gives slightly better results than the URANS models there.

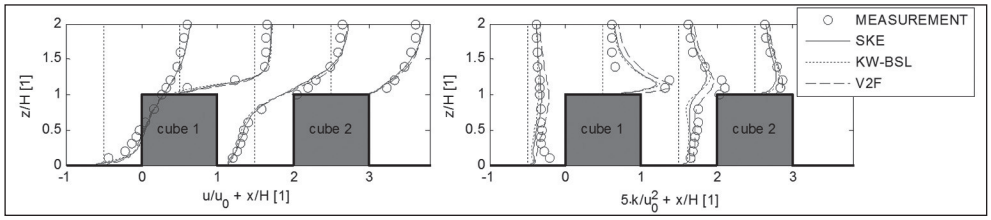

Fig. 3: x-velocity and kinetic energy distribution at the cube 1 and 2 (RANS based models). (Heschl et al., 2010)

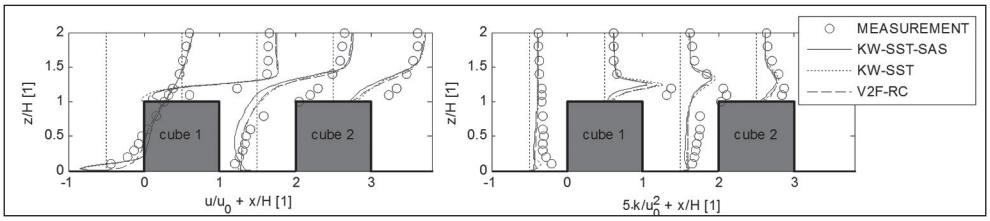

Fig. 4: x-velocity and kinetic energy distribution at the cube 1 and 2 (URANS and SAS based models). (Heschl et al., 2010)

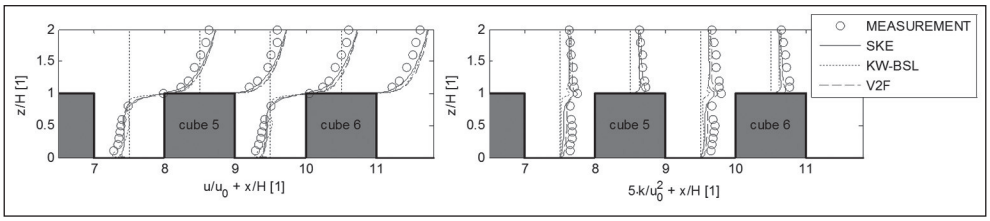

Fig. 5: x-velocity and kinetic energy distribution at the cube 5 and 6 (RANS based models). (Heschl et al., 2010)

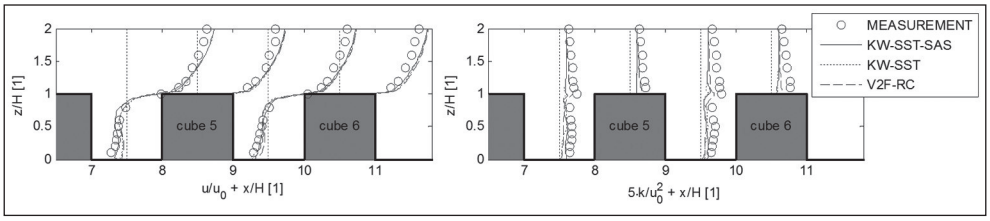

Fig. 6: x-velocity and kinetic energy distribution at the cube 5 and 6 (URANS and SAS based models). (Heschl et al., 2010)

3.3 3D BUILDING ARRAY

In contrast to the cube cases, the third investigated case represents an existing property out of four main buildings with houses and up to 14 m high halls, which geometrical data was generated by simplifing the three-dimensional profile from an airbourne laser scanning. For detailed information it is referred to Meile & Wimmer (2011) and Meile (2011) who carried out laser Doppler anemometry (LDA) and particle image velocemetry (PIV) measurements in a 1:100 scaled wind tunnel experiment. The computational domain was 3.45 m parallel to the wind direction, with a wide of 2 m and height of 1.04 m. The building array is located in the upwind half of the base area including several measurement positions with LDA data (displayed on the left hand side of Fig. 7). The tetrahedral meshes consist out of 2.6 million cells for the y^+=30 grid (cf. right side of Fig. 7) and 6.8 million cells for the y^+=1 grid, which could be achieved by adding 10 rows of densified, near-wall boundary layer cells with a cell-height of 0.0002 m for the first row. The additional non-uniform hexahedral grid with y^+-values of 30 for the wall attached cells was generated out of 2.8 million cells.

For the wind tunnel experiment, the vertical velocity profile upwind the first building is given by $u/u_{ref}=\ln(z/z_0)/\ln(z_{ref}/z_0)$ with the reference velocity u_{ref}=10 m/s at the reference high z_{ref}=0.7 m and the roughness length z_0=0.1 m. The inlet boundary conditions were determined based on measurement data of the mean velocity u in wind direction and the turbulent intensity I with $k=3/2\ (u\ I)^2$, $\varepsilon=c_\mu^{3/4}\ k^{3/2}/l$ and $\omega=\varepsilon/k$, whereby the mixing length l is set to $\min(\kappa\ z, 0.085\ \delta)$ with the boundary layer thickness δ is estimated to the approximated building height of 0.1 m, c_μ=0.09 and κ=0.4187.

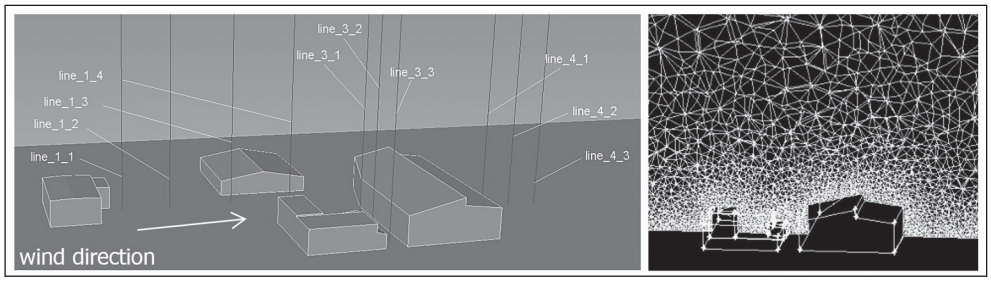

Fig. 7: Investigated building array. Left: Position of lines with LDA data. Right: Tet-grid with y^+=30.

In Fig. 8 profiles of the mean velocity in wind direction from the investigated turbulence models SKE, KW-SST (RANS) and KW-SST-SAS (URANS-SAS) in the y^+=1 grid are compared to the experimental LDA data from Meile & Wimmer (2011). As observed in the cube cases, the predicted velocity profiles downwind single objects do not fit as good into the experimental results as simulated profiles in between or downwind a couple of flow obsticles. At the lines 1-1 and 1-4, leeward the first single building, the agreement with LDA data is not satisfying, although the SKE and KW-SST-SAS reproduce better results than the KW-SST model and the KW-SST-SAS is again able to capture the flow recovery as displayed in Fig. 8, line 1-4. Downstream the building array, at line 4-1 to 4-3, the three tested turbulence models generate alsmost the same velocity profiles, consistent to the experimental data. Between two buildings, at line 3-1 to 3-3, the KW-SST-SAS model delivers the best results, slightly better than both RANS models. The results at line 3-3 and 4-2 are shown examplary in Fig. 8.

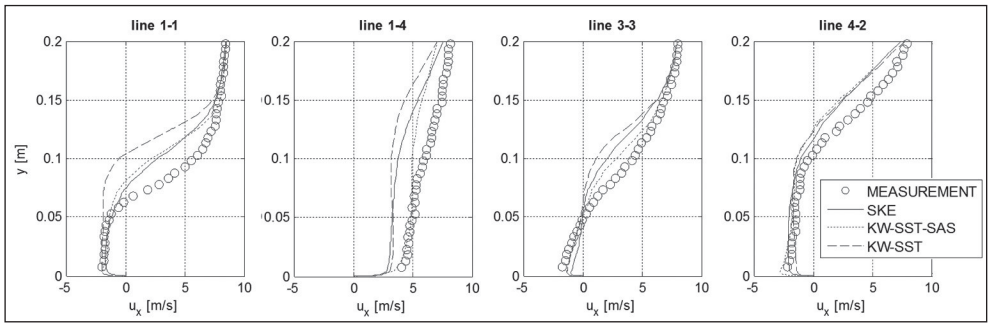

Fig. 8: Downwind velocity component u_x form RANS (SKE, KW-SST) and URANS-SAS (KW-SST-SAS) models in the y^+=1 grid as well as LDA measurements from Meile & Wimmer (2011) along selected lines (cf. Figure 7, left).

In Fig. 9 velocity profiles of the SKE model in the y^+=1 tetrahedral grid (see Fig. 8) are compared to profiles of the SKE model in a tetrahedral and a non-uniform hexahedral y^+=30 grids, to examine the robustness of the prediction in terms of near-wall treatment and grid independency. For all analyzed lines widespread agreement has been observed, expect line 4-2 and 4-3, where small deviations between the simulated results occur (cf. Fig. 9, line 4-2).

Meile (2011) offers two-dimensional contour plots of mean velocity and streamlines from PIV measurement of the wind tunnel experiment. One selected example is compared in Fig. 10 to the results of the SKE model in the tetrahedral mesh with y^+=30. The turbulence model is capable to reproduce the position and size of the recirculation zone quite accurate.

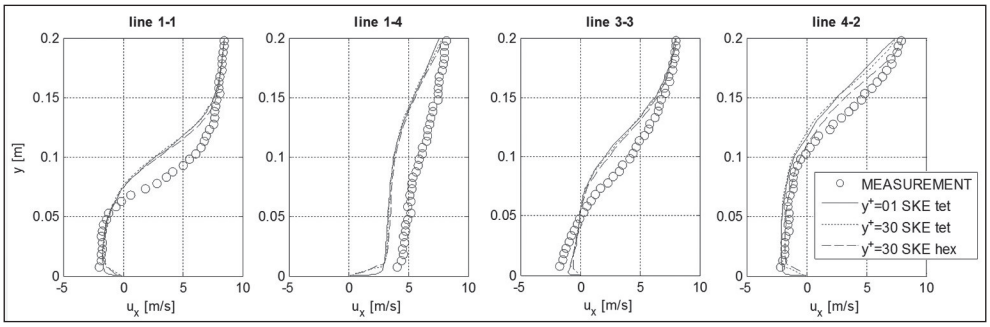

Fig. 9: Downwind velocity component u_x form SKE model variants and experimental LDA data from Meile & Wimmer (2011) along selected lines (cf. Figure 7, left).

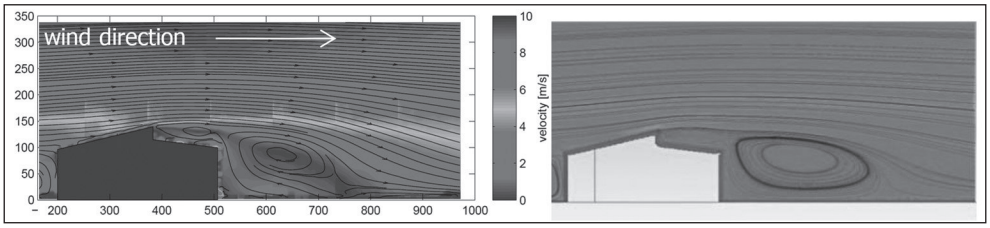

Fig. 10: Contour plot of mean velocity and streamlines in extension of line 3-2 (cf. Figure 7). Left: PIV measurement from Meile (2011). Right: Simulation results from SKE model in y^+=30 tet grid.

4. CONCLUSION

The stagnation point modification for the KW-BSL and the V2F turbulence model was compared with the KW-SST-SAS method and the SKE model to determine prediction quality of airflow around buildings. The investigated test cases contained the flow around a single, three-dimensional cube, a cube array and a building array based on the geometry of an existing property. All models without the stagnation point modification produce too much turbulent kinetic energy which is transported downstream and suppressing an unsteady solution. In addition the high turbulence level dominates the turbulent viscosity distribution in the wake so that the used turbulence models produce similar results. Concerning the building array test cases, an analogue effect has been shown.

If the stagnation point modifications are used the KW-SST and the V2F-RC model switch into unsteady flow (URANS). Compared to the KW-SST-SAS model similar results for the 3D array are achieved. A significant deviation was only observed in the wake of the 3D single cube. In this field the SAS model produces higher velocity fluctuations behind the cube and computes therefore a more realistic recirculation length.

5. ACKNOWLEDGEMENT

The investigations were accomplished by the impulse program “Josef Ressel-Centre” funded by the BMWFJ. Special thanks to Dr. Brown for providing the wind tunnel data.

REFERENCES

Brown, M., Lawson, R., DeCroix, D., Lee, R., 2001. Comparison of Centerline Velocity Measurements Obtained Around 2D and 3D Arrays in a Wind Tunnel. Report LA-UR-01-4138, Los Alamos National Laboratory, Los Alamos.

CEDVAL. Compilation of Experimental Data for Validation of Microscale Dispersion Models, Meteorological Institute, Hamburg University, Germany

Cokljat, D., Kim, S.E., Iaccarino, G., Durbin, P.A., 2003. A comparative assessment of the V2F model for recirculating flows. 41rd AIAA Aerospace Sciences Meeting and Exhibit, Reno, Nevada.

Davidson, L., 2006. Evaluation of the SST-SAS Model: Channel flow, Asymmetric Diffuser and Axi-symmetric Hill. European Conference on Computational Fluid Dynamics, ECCOMAS CFD.

Durbin, P.A., 1995a. Separated flow computations with the k-ε-v2 model. AIAA J. 33, 659-664

Durbin, P.A., 1995b. On the k-ε stagnation point anomaly. International Journal of Heat and Fluid Flow, Vol. 17, pp. 89-90.

Ehrhard, J., 1999. Untersuchung linearer und nichtlinearer Wirbelviskositätsmodelle zur Berechnung turbulenter Strömungen um Gebäude, VDI Verlag GmbH, Deutschland.

Fluent, 2009. FLUENT 14.5 User's Guide. Fluent Inc. Centerra Ressource Park, Lebanon.

Haase, W., Braza, M., Revell, A., 2009. DESider – A Euoropean Effort on Hybrid RANS-LES Modelling. Springer, Berlin Heidelberg.

Heschl, Ch., Sanz, W., Lindmeier, I., Clauss, G., 2010. Validation of scale-adaptive and elliptic relaxation turbulence models applied to flow around buildings, The Fifth International Symposium on Computational Wind Engineering, North Carolina, USA

Lien, F., Kalitzin, G., 2001. Computations of transonic flow with the v2f turbulence model. International Journal of Heat and Fluid Flow, Vol. 22, pp. 53-61.

Lien, F., Yee, E., 2004. Numerical modeling of the turbulent flow developing within and over a 3-D building array, Part I: A high-resolution Reynolds-Averaged Navier-Stokes approach. Journal of Boundary-Layer Meteorology 112, 427-466.

Lopes da Costa, J.C., Castro, F.A., Palma, J.M., 2007. Models for Computer Simulation of Wind Flow over Sparsley Forested Regions. Wind Energy, Springer, Berlin Heidelberg.

Meile, W. & Wimmer, E., 2011. Windkanaluntersuchungen an Gebäudemodellen Teil 2: LDA, Institut für Strömungslehre und Wärmeübertragung, Technische Universität Graz, Austria

Meile, W., 2011. Windkanaluntersuchungen an Gebäudemodellen Teil 1: PIV, Institut für Strömungslehre und Wärmeübertragung, Technische Universität Graz, Austria

Menter, F.R., 1993. Zonal Two Equation k-ω Turbulence Models for Aerodynamical Flows. AIAA paper No. 93-2906, 24th Fluid Dynamics Conference, Florida, 1-21.

Menter, F.R., 1994. Two-Equation Eddy-Viscosity Turbulence Models for Engineering Applications. AIAA Journal, Vol. 32, No. 8, pp. 1598 – 1605.

Menter, F.R., Egorov, Y., 2005. A Scale-Adaptive Simulation Model using Two-Equation Models. 43rd AIAA Aerospace Sciences Meeting and Exhibit, Reno, Nevada.

Menter, F.R., Egorov, Y., 2009. Formulation of the Scale-Adaptive Simulation (SAS) Model during the DESIDER Project. In: Haase, W., Braza, M., Revell, A., (eds.). DESider – A Euoropean Effort on Hybrid RANS-LES Modelling. Springer, Berlin Heidelberg.

Spalart, P., Jou, W.-H., Strelets, M., Allmaras, S., 1997. Comments on the feasibility of LES for wings and on the hybrid RANS/LES approach. In: Liu, C., Liu, Z., Sakell, L., (eds.). Advances in DNS/LES, pp. 137-148. Greden Press.

Strelets, M., 2001. Detached Eddy Simulation of massively separated flows. AIAA Paper 2001-879.

Sveningsson, A., 2003. Analysis of the Performance of Different v2-f Turbulence Models in a Stator Vane Passage Flow. PhD thesis, Chalmers University of Technology, Göteborg, Sweden.